

An exact solution approach for an electric bus dispatch problem

Matías Alvo, Gustavo Angulo, Mathias A. Klapp*

School of Engineering, Pontificia Universidad Católica de Chile, Santiago, Chile

ARTICLE INFO

Keywords:

Electric vehicles
Vehicle scheduling
Charger scheduling
Integer programming
Benders' decomposition

ABSTRACT

We study how to efficiently plan a bus dispatch operation within a public transport terminal working with a mixed fleet of electric and diesel buses and a restricted number of chargers. To meet the daily trip demand, the terminal dispatcher has to assign a trip schedule and a battery charge plan to each bus and also feasibly sequence charging tasks at each charger. We model this problem as an extension of the Vehicle Scheduling Problem, which we later reformulate via a Benders' type decomposition approach into two sub-problems; (1) a master problem assigning bus trip schedules and (2) a satellite problem sequencing charging tasks for a given set of bus trip schedules. Our exact decomposition approach dynamically injects feasibility cuts into the branch-and-bound tree to remove bus trip schedules leading to an infeasible bus charging operation. We assess the effectiveness of our approach and its advantage over a single-stage model in computational experiments inspired by a bus operator from Santiago, Chile. Finally, we provide several managerial insights for planners such as the marginal benefit per additional charger or electric bus and the value added by a mixed fleet compared to a pure electric one.

1. Introduction

Nowadays, it is urgent to replace fossil fuels by renewable energy sources. According to OECD (2016), air pollution caused nearly three million premature deaths in 2010 and might reach up to 6–9 million deaths per year in 2060. Among all air pollutant activities, the urban transportation sector is responsible for approximately 54% of CO and 14% of CO₂ emissions worldwide (Sokhi, 2011). To reduce pollution, some public transport authorities have transitioned to the use of cleaner vehicles, such as electric buses (UITP, 2019). For example, the adoption of electric vehicles in China's public transport systems reached roughly 400 thousand units in 2019 and represented 99% of the world's electric bus fleet (Margolis, 2019). According to Scriven (2019), over 5000 electric buses will be delivered yearly to Latin America by 2025.

Also, a transition towards an electric fleet can be profitable in the long run. According to Heid et al. (2017), the total cost of ownership for electric city buses could equate that of diesel ones as early as 2023. Compared to a diesel vehicle, the purchase of an electric bus is approximately 63% more expensive, but fuel and maintenance costs per vehicle-mile are approximately 3.3 and 2 times cheaper, respectively (Quarles et al., 2020).

Operating electric buses cost-efficiently is also crucial to achieve long-run profitability and pollution reduction. Compared to diesel vehicles, this technology has limited driving ranges and relatively long battery charging times (Pollet et al., 2012). If these restrictions are left out from the operations planning process, one may overestimate the potential usage of an electric fleet at a public transport terminal (depot).

* Corresponding author.

E-mail addresses: malvo1@uc.cl (M. Alvo), gangulo@ing.puc.cl (G. Angulo), maklapp@ing.puc.cl (M.A. Klapp).

1.1. Literature review

Recently, several research efforts within the Transportation Science and Logistics literature have studied strategic and tactical decisions related to the effective and efficient management of electric vehicle fleets and their charging infrastructure. Decisions studied involve the definition of battery capacities (Kunith et al., 2017), charging infrastructure investments (Kunith et al., 2017; Rogge et al., 2018; Wang et al., 2017; Xylia et al., 2017), vehicle purchase decisions (Li et al., 2019; Rogge et al., 2018), and charging station location (Kunith et al., 2017; Wang et al., 2017; Xylia et al., 2017), among others.

The daily bus dispatch operation at a terminal can be modeled as a Vehicle Scheduling Problem (VSP) introduced by Foulkes et al. (1954), which plans the assignment of a sequence of trips (**trip schedule**) to be covered by each vehicle. Each bus can serve one trip at-a-time and each trip is encoded as a time interval that must be assigned to a single vehicle. The single-depot VSP for diesel buses is a special case of the Minimum Cost Network Flow Problem model and is thus efficiently solvable. The authors in Bodin et al. (1983) provide a survey on the VSP and its extensions. More research on the VSP is discussed in Bunte and Klierer (2009), Desaulniers et al. (1998), Desrosiers et al. (1995) and Freling and Paixão (1995).

To improve the utilization of electric buses, one has to integrate battery charging operations into bus dispatch planning. This gives rise to the Electric Vehicle Scheduling Problem (E-VSP) introduced by Wen et al. (2016). Besides assigning trip schedules to buses, a feasible solution to the E-VSP must plan a **battery charge schedule** for each bus, which is a list of charging tasks that ensure a feasible battery operation within its acceptable state of charge (SoC) range; an out-of-range battery usage can significantly reduce its lifespan (Millner, 2010).

The E-VSP is even more complex if we restrict the number of simultaneous charging tasks occurring at the terminal. Such a constraint is required when there exists a fixed number of chargers per charging station or a maximum grid power capacity (Etezadi-Amoli et al., 2010; Pelletier et al., 2016). In this case, a feasible solution must also select and sequence the list of battery charging tasks carried out in each charger, i.e., a **charger schedule**. Similar synchronization constraints are studied for the Vehicle Routing Problem in Drexel (2012).

Therefore, the E-VSP with a restricted number of simultaneous charging tasks has three interlocked decisions: (1) planning feasible trip schedules for each bus covering all trips; (2) designing feasible battery charge schedules for each bus; and (3) assigning and sequencing charger schedules to each charger.

Problems exhibiting a hierarchical structure among decisions, such as the E-VSP, might be amenable to decomposition approaches such as Benders' decomposition (Benders, 2005). This method has been successfully tested in problems arising in a wide range of applications (Rahmaniani et al., 2017) including transportation and logistics problems. Moreover, the Combinatorial Benders' (CB) approach introduced by Codato and Fischetti (2006) extends the ideas of Benders' decomposition to a class of mixed-binary decision problems.

The literature regarding the E-VSP is summarized in Table 1. An initial work by Li (2014) studies an E-VSP for electric buses equipped with battery swap technology. The approach assumes full battery charges with constant charging time. The problem is formulated over a time-expanded network and solved via column-generation. A similar research effort conducted by Adler and Mirchandani (2016) investigates on a VSP for alternative fuel vehicles with limited autonomy; it is assumed that these vehicles may be charged instantaneously.

A first study on E-VSP models that considers partial battery charges is found in Wen et al. (2016). In this work, the energy added to the battery in each charge is modeled as a linear function of charging time. The problem is formulated as a mixed-integer linear programming (MIP) model and solved heuristically. Another related work is proposed by the authors in van Kooten Niekerk et al. (2017). This project models the energy added to the battery in each charge as a non-linear function of charging time. To do so, the authors discretize each battery's SoC level and later build an expanded network in which each node represents a bus starting a trip with a particular SoC level. Partial battery charges are also modeled in Yıldırım and Yıldız (2021), which addresses a problem that simultaneously considers bus fleet composition and scheduling decisions. They propose a column generation approach to solve it, for which they also discretize each battery's SoC level. In all the previous articles, the number of charges simultaneously occurring at any given moment is unrestricted and thus it is impractical for cases in which the number of chargers is restricted.

Recent research projects add limits to the number of vehicles charging in parallel. For example, the authors in Sassi and Oulamara (2016) study an E-VSP restricted to a maximum power consumed from the grid. The problem is formulated as a discrete-time horizon MIP model, in which the energy consumed in each time period is restricted. Two heuristic methods are proposed for large-sized instances of the problem. The approach of Rinaldi et al. (2018) directly limits the number of parallel charges. These authors also discretize time in their model and assume that full charges take less than one time period. A continuous-time model with limited parallel charges is proposed by Rogge et al. (2018); it only considers full battery charges and is heuristically solved via a genetic algorithm.

Additional work on the E-VSP is made in Tang et al. (2019), which designs a robust plan for trip demands with stochastic duration, and in Perumal et al. (2020), which integrates the E-VSP model with crew scheduling decisions. Both efforts deal with complex models and restrict their approach to full battery charges. A final research effort is conducted in Guo et al. (2019), which devises a genetic algorithm to solve a multi-depot E-VSP.

The VSP is not the only transportation model that has been redefined to include additional decisions and constraints required by the operation of electric vehicles. Particularly, the Electric Vehicle Routing Problem (E-VRP) extends the VRP to an operation including electric vehicles. In the VRP, a set of minimum cost routes must be designed to cover a list of customer visits. Besides typical VRP constraints that meet vehicle capacity constraints and customer service time windows, electric vehicle routes must also be planned to have feasible SoC levels at all times. It also may be required to schedule intermediate battery charges within a route.

Table 1
Summary of related literature to the E-VSP.

Reference	Charge time decisions	Partial charges	Limited parallel charging	Continuous time model	Solution approach(es)
Li (2014)			✓		Column generation
Adler and Mirchandani (2016)				✓	Column generation, heuristic
Wen et al. (2016)	✓	✓		✓	Direct MIP, heuristic
Sassi and Oulamara (2016)	✓	✓	✓		Direct MIP, heuristic
van Kooten Niekerk et al. (2017)	✓	✓			Direct MIP, column generation
Rogge et al. (2018)	✓		✓	✓	Heuristic
Rinaldi et al. (2018)			✓		Direct MIP
Tang et al. (2019)			✓		Column generation
Li et al. (2019)	✓		✓		Direct MIP
Perumal et al. (2020)				✓	Heuristic
Yıldırım and Yıldız (2021)	✓	✓		✓	Column generation
This work	✓	✓	✓	✓	Cut generation

E-VRPs only considering full battery charges of constant duration are studied in [Andelmin and Bartolini \(2017\)](#), [Andelmin and Bartolini \(2019\)](#), [Bruglieri et al. \(2019a\)](#), [Bruglieri et al. \(2019b\)](#), [Erdoğan and Miller-Hooks \(2012\)](#), [Koç and Karaoglan \(2016\)](#) and [Montoya et al. \(2016\)](#). More E-VRP models considering full battery charges with variable charging times depending on the battery SoC level are found in [Goeke and Schneider \(2015\)](#), [Schneider et al. \(2014\)](#) and [Hiermann et al. \(2016\)](#). Recently, more efforts on the E-VRP have considered partial battery charges. For instance, the authors in [Felipe et al. \(2014\)](#), [Desaulniers et al. \(2016\)](#) and [Keskin and Çatay \(2018\)](#) consider linear energy charges as a function of charging time. Also, [Froger et al. \(2019\)](#), [Froger et al. \(2021\)](#), [Montoya et al. \(2017\)](#) and [Koç et al. \(2019\)](#) study piecewise linear approximations for battery charges as a function of time. Finally, [Lee \(2020\)](#) proposes a generic model for any concave and non-decreasing function of time. Perhaps, the more complete E-VRP project in terms of the generality of decisions and restrictions involved is found in [Froger et al. \(2021\)](#). This work develops a method to design customer visiting routes for each electric vehicle within a fleet. Each route may include or not charging tasks assigned to a specific charging station. It considers a maximum number of parallel charges per station, admits partial battery charges and includes a piecewise linear relation between charge time and the energy injected to each bus battery. The authors present an extended path-based formulation, which is solved via a two-stage matheuristic. In the first stage, promising routes are generated for each vehicle without considering charging station capacities. Later, combinatorial cuts are introduced to discard first-stage solutions for which a feasible charger schedule cannot be found. However, in their computational experiments, the authors present a setting in which parallel charging constraints appear to be frequently not binding. In one set of experiments, the authors consider best known solutions for instances of an E-VRP with unlimited chargers generated by [Montoya et al. \(2017\)](#) and then add an additional capacity constraint considering one or two chargers per station. For a capacity of one charging station, their solution results in an infeasible schedule in 53 of 119 instances; in four cases a larger number of routes were required. For a capacity of two, just 12 out of 120 solutions were infeasible, and in just one case additional routes were needed.

To the best of our knowledge, there is no research effort regarding exact approaches for the E-VSP or related transportation problems operating with electric vehicles that considers charging task sequencing and duration decisions, and restricts the number of vehicles charging in parallel over a continuous time horizon. Furthermore, no exact decomposition approach has been proposed for the E-VSP.

1.2. Scope and contribution

In this article, we study how to plan a bus dispatch operation within a public transport terminal working with a mixed fleet of electric and diesel buses. Our approach is novel, since it extends the existing E-VSP models within the literature with several features. It is the first study that optimally designs trip and battery charge schedules for each bus and simultaneously sequences charging tasks at each charger in a continuous-time horizon. It also considers a restricted number of chargers and makes fully flexible charge duration decisions.

The objective function chosen is to hierarchically minimize (1) the number of additional diesel buses pulled out from the terminal each day subject to a fixed electric fleet and (2) their total energy consumed over the day. This choice of objective aims to minimize pollution, but the approach is flexible enough to work with any objective as a function of trip schedules.

Additional contributions are summarized below:

- We propose a novel MIP formulation for the E-VSP model and an exact solution framework that together exploit the problem structure and decompose decisions into two natural sub-problems: (1) a master problem assigning trip and battery charge schedules for each bus and (2) a satellite problem that identifies a feasible charger schedule for a given set of bus trip schedules or, otherwise, deduces a feasibility cut that prunes the current trip schedule leading to an infeasible bus charging operation. These cuts are dynamically injected to the branch-and-bound tree.
- Our approach customizes the Combinatorial Benders' decomposition method to our problem in two different ways. First, it adds problem-specific feasibility cuts by lifting traditional “no-good cuts” and exploiting the structure of a feasible trip schedule. Also, it tightens the feasible domain of the first-stage model by including an auxiliary structure that couples first-stage solutions with relaxed charger schedules.

- We assess the effectiveness of our solution method and its advantage over a direct MIP model in computational experiments inspired by a bus operator from Santiago, Chile.
 - Tactical fleet planning and infrastructure investment decisions may also benefit from our study.
- We provide several managerial insights, such as an estimate of the marginal benefit provided by an additional charger or electric bus. Also, we discuss how the inclusion of diesel vehicles can add operational flexibility and improve electric fleet utilization.

The remainder of this article is organized as follows. Section 2 describes the problem addressed and main assumptions considered. Section 3 presents the mathematical formulation of the exact two-stage approach. Section 4 describes the numeric studies conducted, presents results and draws managerial insights. Finally, Section 5 concludes the study and proposes future research.

2. Problem statement

We consider the bus dispatch operation of a single public transport terminal, *a.k.a.*, depot, over a 24-h time horizon. Before the operation starts, the terminal's dispatcher is given a set T of trip services to be executed throughout the day, where each trip $j \in T$ specifies its start and end time at the depot given by t_j^{start} and t_j^{end} , respectively. The dispatcher has to plan a feasible trip coverage and guarantee that each trip is executed by exactly one bus from the terminal's available fleet represented by a set V . Each bus is electric or diesel and serves at most one trip at-a-time. We assume that all electric vehicles are homogeneous models with homogeneous batteries, but can start the day with different levels of battery charge. Thus, let V_0 be the set of all available electric buses and $V_1 = \{v_1\}$ be a singleton representing all available diesel buses, *i.e.*, $V := V_0 \cup V_1$. The maximum number of available diesel buses is defined as \bar{d}^{max} .

Executing trip $j \in T$ consumes \bar{e}^j SoC units from an electric bus battery or an amount γ_j of diesel fuel; these parameters are not necessarily proportional to trip distance or duration since other effects, such as traffic congestion and road degree, might affect consumption. Each electric bus $i \in V_0$ starts the day with a SoC level \bar{e}_i and must end the day with a SoC level no smaller than \bar{e}^{end} to ensure sustainable day-to-day operations. At all times, a vehicle's battery SoC level must lie within a feasible range defined by $[\bar{e}^{\text{min}}, \bar{e}^{\text{max}}]$.

An electric bus can charge its battery in one charger within an homogeneous set C installed at the depot. Each charger $c \in C$ can serve at most one bus at-a-time, charge its battery at a rate of f SoC units per minute, and operate within the time interval $[p^{\text{start}}, p^{\text{end}}]$, which may be the whole day or a sub-period where electricity is cheaper at the terminal. In our problem setting, we take charging start time and duration as decision variables. We also assume that each bus can only be charged once between the execution of consecutive trips. Also, we assume a constant SoC charging rate as a function of the charging task's duration. This is a limitation of our model, since the relationship between energy injected and charge time is in reality a concave function. However, it is common in the E-VSP and E-VRP literature to approximate it with a linear function. Finally, we assume that diesel buses start with sufficient fuel to cover their daily operation or, equivalently, can refuel instantaneously.

The problem studied in this work aims to simultaneously plan trip, battery charge and charger schedules meeting trip coverage, operational bus constraints, parallel charging capacity at the depot and feasible SoC levels for each electric bus battery. We set as objective to hierarchically minimize the number of diesel buses pulled out from the depot first and later the total consumption of diesel buses.

3. Two-stage model formulation

Now, we formulate a two-stage MIP model for the electric bus dispatch problem stated in Section 2. An alternative formulation is the single-stage model defined in Appendix D. We chose the two-stage formulation, since according to Drexler (2012) a single-stage model imposes hard task and resource synchronization constraints. Also, as empirically discussed in Section 4, the computational time of a single-stage formulation rapidly explodes as a function of the number of vehicles, chargers and trips and, thus, it becomes intractable even for some small-sized instances.

Our two-stage formulation is solved exactly using a Benders' type approach, which is equipped with a customized version of CB cuts introduced by Codato and Fischetti (2006). In our first-stage model, we plan a feasible trip and battery charge schedule for each bus, but relax charging task sequencing at each charger and replace these difficult constraints with aggregated restrictions limiting the maximum power delivered per charger at specific time intervals. In turn, we only obtain a relaxation of the original model whose solution might be infeasible for the general setting. We test a first-stage solution potential infeasibility as follows. Each time a feasible trip schedule to the first-stage model is found, we solve a second-stage model that inputs such a schedule and tries to identify a feasible pair of battery charge and charger schedules to the overall problem. If no pair exists, then a feasibility cut is added to the first-stage model to cut-off this specific trip schedule from the first-stage solution space. Even though it is computationally more expensive, recomputing all battery charge schedules in the second-stage model allows us to discard with one cut multiple first-stage solutions having a common trip schedule. Fig. 1 presents a scheme of the proposed two-stage solution approach.

The details of each model are given as follows. The decision variables for the first- and second-stage models are summarized in Tables 9 and 10, respectively, in Appendix A.

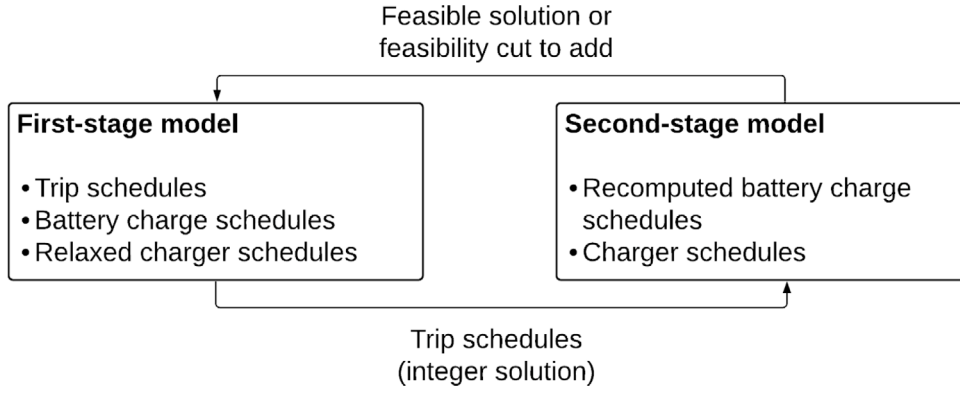


Fig. 1. Scheme of the proposed two-stage solution approach.

3.1. First-stage model

We encode our first-stage solution in a digraph $G = (N, A)$, where the set of nodes $N := T \cup V \cup \{0\}$ is formed by all trips, a source for each electric bus, one source for all diesel buses, and a sink, respectively. Set A contains arc (j_1, j_2) if trips $j_1, j_2 \in T$ can be executed by a single bus (i.e., $t_{j_1}^{\text{end}} \leq t_{j_2}^{\text{start}}$), arc (i, j) for each $i \in V$ and $j \in T$, and arc $(j, 0)$ for each $j \in T$. So, a path in G starting at node $i \in V$ and defined by $\{i, j_1, j_2, \dots, j_p, 0\}$ represents a daily trip itinerary for a bus executing the p trips j_1, j_2, \dots, j_p . To distinguish vehicle types, define set $L := \{0, 1\}$, where type 0 represents electric buses and type 1 diesel ones. Then, define set $A_\ell := \{(u, v) \in A : u \in T \cup V_\ell\}$ as the subset of arcs that buses of type $\ell \in L$ can use. Also, define the set of arcs in A_ℓ leaving and entering node $i \in N$ as $\delta_\ell^+(i) := \{(i, j) \in A_\ell : j \in N\}$ and $\delta_\ell^-(i) := \{(j, i) \in A_\ell : j \in N\}$, respectively.

Each arc $a := (u, v) \in A_0$ also defines a time interval $[\alpha_a, \beta_a]$ when an electric bus covering consecutive trips u and v may charge in between these trips. Accordingly, α_a is set equal to $\max(p^{\text{start}}, t_u^{\text{end}})$ if $u \in T$ and to p^{start} otherwise, while β_a is set equal to $\min(p^{\text{end}}, t_v^{\text{start}})$ if $v \in T$ and to p^{end} otherwise. So, let \bar{A}_0 be the set of arcs in which it is possible for a charge to occur, i.e., $\bar{A}_0 := \{a \in A_0 : \alpha_a < \beta_a\} \subseteq A_0$. Also define $I^{\text{start}} := \{\alpha_a : a \in \bar{A}_0\}$ and $I^{\text{end}} := \{\beta_a : a \in \bar{A}_0\}$ as the sets of all interval start and end times, respectively. Finally, let $\bar{\delta}_0^+(i) := \delta_0^+(i) \cap \bar{A}_0$ for $i \in V_0 \cup T$.

Decision Variables

We can now define first-stage decision variables. Let $x_a^\ell \in \{0, 1\}$ be a binary variable defined for each $\ell \in L$ and $a \in A_\ell$ representing a bus of type ℓ traversing arc a . Decision vector \mathbf{x} encodes a set of trip schedules as paths starting from bus nodes in V , visiting a subset of trip nodes in T and ending in node 0. For each electric bus arc $a = (u, v) \in A_0$, we also define a continuous variable $e_a \geq 0$ representing the battery's SoC immediately after a possible battery charge in between nodes u and v if $(u, v) \in \bar{A}_0$ or the remaining SoC in the bus battery immediately after leaving node u if $(u, v) \notin \bar{A}_0$. So, decision vector \mathbf{e} encodes battery SoC levels for electric buses. We also define a binary variable $y_a^c \in \{0, 1\}$ and a continuous variable $g_a^c \geq 0$ for each arc $a \in \bar{A}_0$ modeling whether or not a charge occurs and the SoC level injected to the battery at charger $c \in C$, respectively.

A graphic example of a first-stage problem graph is depicted in Fig. 2.

Objective function

In general, our decomposition approach works for any linear objective function on variables \mathbf{x} . We chose to minimize two objectives in a hierarchical order. The first objective is to minimize the total number of diesel buses used in the operation as stated in (3.1a). The second objective is to minimize the total energy consumed by all diesel buses (3.1b). We initially solve our two-stage model with objective (3.1a) in the first-stage. When termination conditions are met, we set the number of diesel vehicle pullouts equal to the objective value found and re-solve our model with objective (3.1b).

$$\min \sum_{a \in \bar{\delta}_1^+(v_1)} x_a^1, \quad (3.1a)$$

$$\min \sum_{a=(u,v) \in A_1 : v \neq 0} \gamma_v \cdot x_a^1. \quad (3.1b)$$

First-stage feasibility constraints

Any value of $(\mathbf{x}, \mathbf{e}, \mathbf{y}, \mathbf{g})$ satisfying system (3.2) is feasible to the first-stage model.

$$\sum_{\ell \in L} \sum_{a \in \delta_\ell^-(j)} x_a^\ell = 1, \quad \forall j \in T, \quad (3.2a)$$

$$\sum_{a \in \bar{\delta}_0^+(i)} x_a^0 \leq 1, \quad \forall i \in V_0, \quad (3.2b)$$

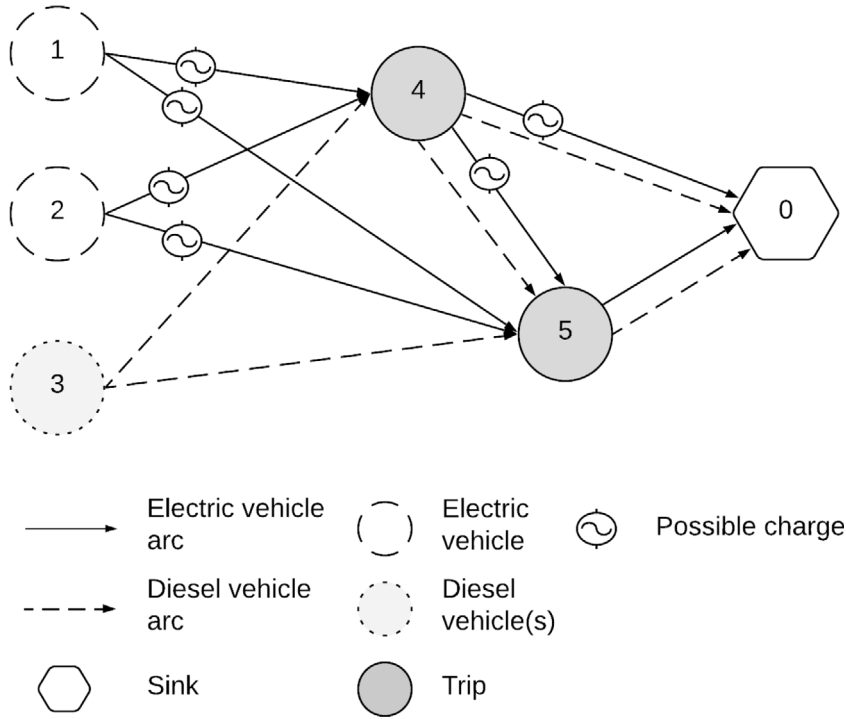


Fig. 2. Example of a first-stage problem graph for an instance with two trips, two electric buses and one or more diesel buses.

$$\sum_{a \in \delta_1^+(v_1)} x_a^1 \leq \bar{d}^{\max}, \quad (3.2c)$$

$$\sum_{a \in \delta_\ell^+(j)} x_a^\ell - \sum_{a \in \delta_\ell^-(j)} x_a^\ell = 0, \quad \forall j \in T, \ell \in L, \quad (3.2d)$$

$$e_a - \bar{e}_i \cdot x_a^0 = \sum_{c \in C} g_a^c, \quad \forall i \in V_0, a \in \delta_0^+(i), \quad (3.2e)$$

$$e_a - \bar{e}_i \cdot x_a^0 = 0, \quad \forall i \in V_0, a \in \delta_0^+(i) \setminus \bar{\delta}_0^+(i), \quad (3.2f)$$

$$\sum_{a \in \delta_0^+(j)} e_a - \sum_{a \in \delta_0^-(j)} e_a = \sum_{a \in \delta_0^+(j)} \sum_{c \in C} g_a^c - \bar{e}^j \cdot \sum_{a \in \delta_0^-(j)} x_a^0, \quad \forall j \in T, \quad (3.2g)$$

$$(\bar{e}^{\min} + \bar{e}^j) \cdot x_a^0 \leq e_a, \quad \forall j \in T, a \in \delta_0^-(j), \quad (3.2h)$$

$$\bar{e}^{\text{end}} \cdot x_a^0 \leq e_a, \quad \forall a \in \delta_0^-(0), \quad (3.2i)$$

$$e_a \leq \bar{e}^{\max} \cdot x_a^0, \quad \forall a \in A_0, \quad (3.2j)$$

$$\sum_{c \in C} y_a^c \leq x_a^0, \quad \forall a \in \bar{A}_0, \quad (3.2k)$$

$$g_a^c \leq \min(f \cdot (\beta_a - \alpha_a), \bar{e}^{\max} - \bar{e}^{\min}) \cdot y_a^c, \quad \forall a \in \bar{A}_0, c \in C, \quad (3.2l)$$

$$\sum_{a \in \bar{A}_0 : [\alpha_a, \beta_a] \subseteq [t_1, t_2]} g_a^c \leq f \cdot (t_2 - t_1), \quad \forall c \in C, t_1 \in I^{\text{start}}, t_2 \in I^{\text{end}} : t_1 < t_2, \quad (3.2m)$$

$$x_a^l \in \{0, 1\}, \quad \forall l \in L, a \in A_l, \quad (3.2n)$$

$$y_a^c \in \{0, 1\}, \quad \forall a \in \bar{A}_0, c \in C, \quad (3.2o)$$

$$e_a \geq 0, \quad \forall a \in A_0, \quad (3.2p)$$

$$g_a^c \geq 0, \quad \forall a \in \bar{A}_0, c \in C. \quad (3.2q)$$

Constraints (3.2a) guarantee that all trips are executed by exactly one vehicle. Constraints (3.2b), (3.2c) and (3.2d) enforce vehicle flow conservation constraints for each vehicle starting from node $i \in V$. Constraints (3.2e), (3.2f) and (3.2g) impose battery SoC flow conservation for each node. Constraints (3.2h), (3.2i) and (3.2j) guarantee that battery SoC is kept within feasible ranges. Constraints (3.2k) allow charges only in arcs traversed by electric vehicles, whereas constraints (3.2l) impose feasible charging

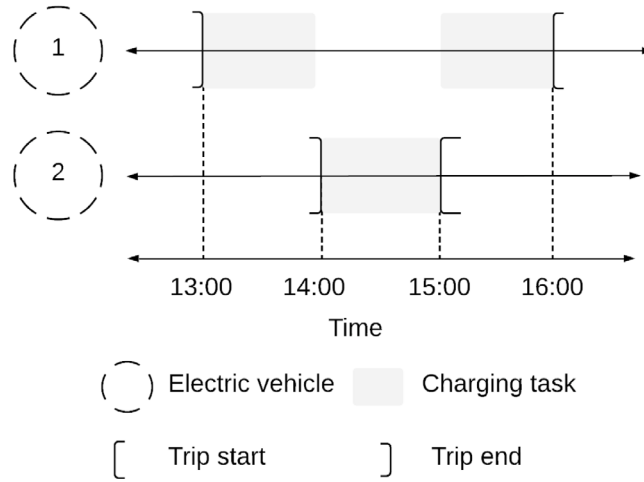


Fig. 3. Example of a first-stage feasible solution for a problem instance with two electric buses and one charger.

ranges. Then, constraints (3.2m) guarantee that the total power charged from each charger within each time interval $[t_1, t_2]$ is always less than or equal to its power capacity. Not all constraints (3.2m) are required, since one constraint for a specific time interval $[t_1, t_2]$ may be implied by one or more constraints over smaller time intervals contained within $[t_1, t_2]$. In particular, if for $t_1, t'_1 \in I^{\text{start}}$ and $t_2, t'_2 \in I^{\text{end}}$, we have that $[t_1, t_2] \subset [t'_1, t'_2]$ and that the sets of time intervals $[\alpha_a, \beta_a]$ for $a \in \bar{A}_0$ contained in each of $[t_1, t_2]$ and $[t'_1, t'_2]$ are the same, then the constraint imposed by $[t'_1, t'_2]$ is redundant, and thus removed from our formulation. Finally, constraints (3.2n)–(3.2q) define variable domains.

In the first-stage model, constraints (3.2m) guarantee to meet charger power capacities, but do not ensure non-preemptive bus-to-charger assignments. Therefore, it is possible that the first-stage solution yields an infeasible solution to the overall problem. Fig. 3 illustrates an example of a first-stage solution infeasible for the overall two-stage model. It presents a three-hour operation at one charger, in which two buses require to charge: bus 1 requires a 120 minute charge and bus 2 a 60 min one. We observe that constraints (3.2m) allow us to schedule two charges for bus 1 interrupted by the charge for bus 2. However, this schedule is infeasible, since each charging task must be uninterruptedly performed. In this case, bus 2 is forced to charge between 14:00 and 15:00 and thus bus 1 cannot charge more than 60 continuous minutes.

3.2. Second-stage model

We now present the second-stage model whose function is to identify feasible battery charge schedules and schedules for each charger that certify the feasibility of a particular set of trip schedules or to prove infeasibility, otherwise. Although the first-stage solution also identifies battery charge schedules for each bus, we only fix vector \mathbf{x} in the second stage and recompute all remaining decisions. This choice allows us to test feasibility of multiple first-stage solutions with identical \mathbf{x} values in a single solution of the second-stage model; it is correct if the first-stage objective depends only on vector \mathbf{x} .

As diesel buses do not require charging, the second-stage model only considers electric buses having at least one trip assigned in the first-stage model. For each electric bus i , define \hat{d}_i as the number of possible charging tasks available within its schedule. Recall that \hat{d}_i is equal to the number of arcs in \bar{A}_0 traversed by bus i in the first-stage solution. Each possible charging task $d \in \{1, \dots, \hat{d}_i\}$ defines an interval $[\hat{\alpha}_{i,d}, \hat{\beta}_{i,d}]$ where a charge may occur. Also, let $\rho_{(i,d)}$ be the cumulative SoC level consumed by bus i minus its initial SoC immediately before its $(d+1)$ -th possible charging task or the end of its schedule if $d = \hat{d}_i$.

The second-stage model is built over a digraph $H = (\Omega, \Gamma)$, where set Ω contains nodes (i, d) , each representing the d -th possible charging task for bus i , a source node \underline{S} and a sink \bar{S} . In set Γ , we add an arc $((i_1, d_1), (i_2, d_2))$ for each pair of different charging tasks $(i_1, d_1) \neq (i_2, d_2)$ if the d_1 -th possible charge of bus i_1 and the d_2 -th possible charge of bus i_2 can be consecutively carried out in one charger, i.e., $\{(i_1, d_1), (i_2, d_2) : (i_1, d_1) \neq (i_2, d_2), \hat{\alpha}_{i_1, d_1} < \hat{\beta}_{i_2, d_2}\}$. Additionally, we add to Γ a source arc $(\underline{S}, (i, d))$ and sink arc $((i, d), \bar{S})$ for each $(i, d) \in \Omega$. Therefore, an \underline{S} – \bar{S} path in H given by $\{\underline{S}, (i_1, d_1), (i_2, d_2), \dots, (i_q, d_q), \bar{S}\}$ represents a sequence of q charging tasks executed by a single charger. The set of arcs leaving \underline{S} is denoted by $\Gamma_{\underline{S}}^+$. Also, define $\Gamma_{(i,d)}^+$ and $\Gamma_{(i,d)}^-$ as auxiliary subsets containing the arcs entering and leaving node (i, d) , respectively, and define $\phi_{(i,d),(i',d')} := \min\{(\min\{\hat{\beta}_{i',d'}, \hat{\beta}_{i,d}\} - \hat{\alpha}_{i,d}) \cdot f, (\bar{e}^{\max} - \bar{e}^{\min})\}$ as the maximum charge allowed for task (i, d) if it is scheduled at a charger immediately before task (i', d') . Finally, let $\mathbb{I}(i, d)$ be an indicator function equal to 1 if $d = \hat{d}_i$ and 0, otherwise, for each $i \in V_0$ and $d \leq \hat{d}_i$. Fig. 4 presents an example of how charging tasks and parameters $\hat{\alpha}$, $\hat{\beta}$ and ρ are defined for a particular vehicle and trip schedule.

Decision Variables

In the second-stage model, we define continuous variables $v_{i,d} \geq 0$ and $b_{i,d} \geq 0$ representing the amount charged and start time for the d th possible charge of bus i , respectively. Moreover, we define a binary variable $z_a \in \{0, 1\}$ for each arc $a \in \Gamma$ to encode

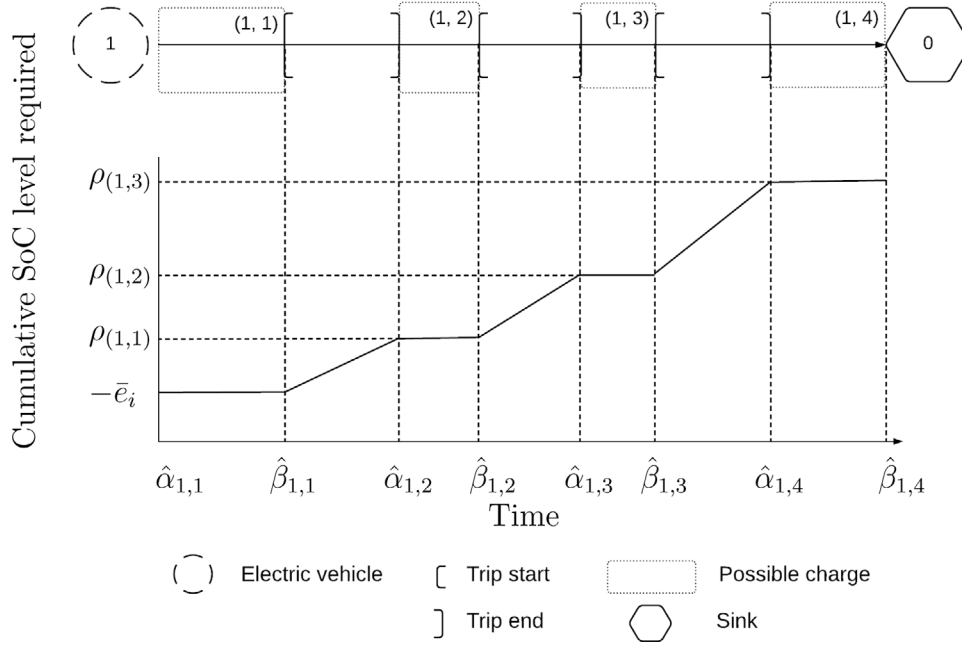


Fig. 4. Example of the definition of charging tasks in the second-stage problem for an electric vehicle trip schedule with three trips.

chargers assignment and sequencing. In particular, for $a = ((i_1, d_1), (i_2, d_2)) \in \Gamma$, variable $z_{(i_1, d_1), (i_2, d_2)}$ represents whether possible charging tasks (i_1, d_1) and (i_2, d_2) are consecutively executed in one charger. Finally, we define a single non-negative variable $\eta \geq 0$ representing the maximum violation over all constraints in (3.4a).

Second-stage objective function

The objective of the second-stage model is to minimize the maximum violation to constraints in (3.4a). The tested set of electric bus trip schedules is feasible for the overall model if there exists a feasible solution to (3.4) with $\eta = 0$.

$$\min \quad \eta. \quad (3.3a)$$

Second-stage feasibility constraints

$$\sum_{d' \leq d} v_{i,d'} - \rho_{i,d} + \eta \geq \max(\bar{e}^{\min}, \mathbb{I}(i, d) \cdot \bar{e}^{\text{end}}), \quad \forall (i, d) \in \Omega, \quad (3.4a)$$

$$\sum_{d' \leq d} v_{i,d'} - \rho_{i,d-1} \leq \bar{e}^{\max}, \quad \forall (i, d) \in \Omega, \quad (3.4b)$$

$$v_{i,d} \leq \sum_{a \in \Gamma_{(i,d)}^+} \phi_a \cdot z_a, \quad \forall (i, d) \in \Omega, \quad (3.4c)$$

$$\sum_{a \in \Gamma_{(i,d)}^+} z_a = \sum_{a \in \Gamma_{(i,d)}^-} z_a, \quad \forall (i, d) \in \Omega, \quad (3.4d)$$

$$\sum_{a \in \Gamma_{(i,d)}^-} z_a \leq 1, \quad \forall (i, d) \in \Omega, \quad (3.4e)$$

$$\sum_{a \in \Gamma_{\bar{\Sigma}}^+} z_a \leq |C|, \quad (3.4f)$$

$$b_{i,d} + \frac{1}{f} \cdot v_{i,d} \leq b_{i',d'} + (\hat{\beta}_{i,d} - \hat{\alpha}_{i',d'}) \cdot (1 - z_{(i,d),(i',d')}), \quad \forall ((i, d), (i', d')) \in \Gamma, \quad (3.4g)$$

$$\hat{\alpha}_{i,d} \leq b_{i,d}, \quad \forall (i, d) \in \Omega, \quad (3.4h)$$

$$b_{i,d} + \frac{1}{f} \cdot v_{i,d} \leq \hat{\beta}_{i,d}, \quad \forall (i, d) \in \Omega, \quad (3.4i)$$

$$z_a \in \{0, 1\}, \quad \forall a \in \Gamma, \quad (3.4j)$$

$$\eta \geq 0, \quad (3.4k)$$

$$v_{i,d} \geq 0, \quad \forall (i, d) \in \Omega, \quad (3.4l)$$

$$b_{i,d} \geq 0, \quad \forall (i, d) \in \Omega. \quad (3.4m)$$

Constraints (3.4a) and (3.4b) guarantee that SoC levels are within feasible ranges or $\eta > 0$. Constraints (3.4c) allow to charge at task (i, d) only if there exists a corresponding charger schedule containing that task. Constraints (3.4d), (3.4e) and (3.4f) impose charger schedule flow conservation. At most $|C|$ flows are allowed to be created from the source node \underline{s} to meet parallel charging capacity. These constraints assume a homogeneous set of chargers, but can be extended to chargers with heterogeneous charge powers by creating one source node per charger and slightly reformulating the first- and second-stage models. Constraints (3.4g) prohibit consecutive charging tasks in one charger from overlapping. Then, constraints (3.4h) and (3.4i) impose that each possible charge start time occurs within its feasible time interval and that maximum charging amounts are met. Finally, constraints (3.4j)–(3.4m) define variable domains.

The following proposition allows us to eliminate arcs from set Γ without loss of generality.

Proposition 1. *Let $q, q' \in \Omega$ be two possible charging events such that $\hat{\alpha}_q \leq \hat{\alpha}_{q'}$, $\hat{\beta}_q \leq \hat{\beta}_{q'}$. Then, if there exists a feasible solution to (3.4) such that $z_{(q',q)} = 1$, then there exists another feasible solution with the same objective value such that $z_{(q',q)} = 0$.*

The proof is presented in Appendix B. It lies on the fact that if q' directly precedes q on the same charger, then both can be interchanged to obtain another feasible solution. This result allows us to reduce the search space by removing all such arcs (q', q) from Γ .

Dynamic generation of feasibility cuts

When a particular integer solution \bar{x} is proven infeasible for the overall model, then it must be eliminated from the search space of the first-stage model. To do so, we add a “no-good cut” to formulation (3.2) that cuts off solution \bar{x} in the spirit of the CB approach proposed by Codato and Fischetti (2006).

Define sets $X := \{(a, \ell) : \ell \in L, a \in A_\ell, \bar{x}_a^\ell = 1\}$ and $\bar{X} := \{(a, \ell) : \ell \in L, a \in A_\ell, \bar{x}_a^\ell = 0\}$. A CB cut is defined as

$$\sum_{(a,\ell) \in X} (1 - x_a^\ell) + \sum_{(a,\ell) \in \bar{X}} x_a^\ell \geq 1, \quad (3.5)$$

meaning that a solution x satisfying cut (3.5) must differ in at least one component from \bar{x} .

If the second-stage problem has continuous variables only and becomes infeasible for a given binary first-stage solution, Codato and Fischetti (2006) proposes to strengthen the “no-good cut” by finding an irreducible infeasible system. Such a system yields a minimal set of first-stage variables whose current values must be changed in order to restore feasibility of the second-stage problem. In our case, to strengthen (3.5), we observe that the underlying trip schedules for electric vehicles are completely defined by the traversed set of arcs. Therefore, we may lift the cut to

$$\sum_{(a,0) \in X} (1 - x_a^0) \geq 1, \quad (3.6)$$

which is dynamically added in a branch-and-cut fashion to (3.2).

4. Numerical experiments

In this section, we test our model and solution in a family of computational experiments inspired by a bus operator in Santiago, Chile. Our goal is to assess our method’s computational performance and present its computational advantage over a single-stage MIP model. Also, we present several managerial insights obtained from efficient bus dispatch operations.

The program was implemented in Python 3.8.5 with the Gurobi 9.1.2 solver interface. All experiments were executed on a computer with a 6-core Intel Core i7–10710U processor and 32 GB of RAM. The terminating condition for running our two-stage model was set to a time limit of 60 min for each objective.

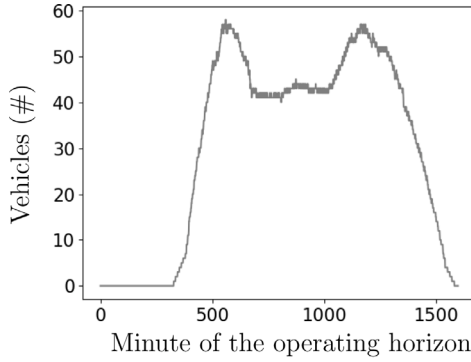
4.1. Dataset and experimental design

We designed a family of problem instances based on real data provided by a bus operator of Santiago’s public transportation system. An instance’s key parameters are presented in Table 2. All instances tested share the same base set of trips, each with a time window, trip duration and consumption information. Trips start and end times were gathered from historic data of a bus service dispatching more than 300 trips per weekday. Fig. 5a presents the number of trips required to be under execution for each minute over the operating horizon. As depicted, the demand pattern has clear morning and afternoon peaks, as it is usual in most public transportation systems. Multiple sets T were drawn from this dataset maintaining the dispersion of trips to be served over time. The SoC consumption per trip is obtained from historic averages measured by an Automatic Vehicle Location (AVL) system. The scatter plot in Fig. 5b illustrates the historic relation between SoC consumption and trip duration. An average trip consumes 20.2% of the battery’s SoC and takes 141 min.

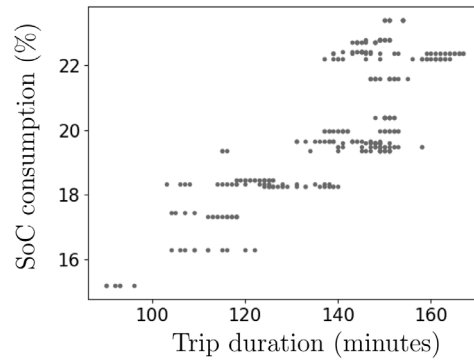
For each set T , we set \bar{d}^{\max} as the minimum number of diesel buses required to cover all trips with a pure diesel fleet; it is pre-computed by solving a VSP model. Then, we set the number of available electric vehicles as $|V_0| := \lceil \bar{d}^{\max} \cdot \%E \rceil$ depending on the target percentage of electric vehicles ($\%E$).

Table 2
Definition of main operational parameters.

Parameter	Definition
$ T $	Number of trips to serve
$ C $	Number of available chargers
\bar{d}^{\max}	Minimum pull-out of diesel vehicles required to cover all trips in absence of the electric fleet
$\%E$	Target percentage of the fleet to be composed by electric vehicles
$ V_0 $	Number of available electric vehicles. Calculated as $\lceil \%E \cdot \bar{d}^{\max} \rceil$
EVA	Relative size of the battery compared to the one used in the base case experiment



(a) Trips required to be under execution per minute of the operating horizon.



(b) SoC consumption and duration for each trip in our data set.

Fig. 5. Description of the base set of trips used for the numerical experiments.

Table 3
Set of KPIs measuring computational performance for each instance.

Metric	Definition
$time_1, time_2$	Total computation time (in s) for the first- and second-level objective, respectively
gap_1	Absolute optimality gap for the first-level objective, as reported by Gurobi
$gap_2^{\%}$	Percentage optimality gap for the second-level objective, as reported by Gurobi
sT_1, sT_2	Total time spent solving the second-stage problem for both objectives
sN_1, sN_2	Number of times the second-stage problem was solved for both objectives
sI_1, sI_2	Number of infeasible first-stage solutions, <i>i.e.</i> , number of CB cuts injected, for both objectives

We set all feasible battery SoC ranges to $\bar{e}^{\min} = 20\%$ and $\bar{e}^{\max} = 100\%$, respectively. In this setting, a fully charged battery provides to the vehicle an autonomy to serve roughly four trips before a charge is needed. Initial SoC levels \bar{e}_i were drawn from a uniform distribution between 20% and 30%. This reflects an operation in which the starting energy of the planning horizon is linked to the end of the previous day. Accordingly, parameter \bar{e}^{end} is set to 25%, *i.e.*, the average between 20% and 30%. As an alternative, we may have assumed that all vehicles have fully charged batteries at the start of the day, meaning that overnight charges occurred for each vehicle. However, we chose a scenario with low energy levels to add operational difficulty to our instances. Also, each charger's power f was set to $1.1 \frac{\%}{\text{minute}}$, which corresponds to the first segment's slope of the piecewise linear approximation for the relation between SoC level charged and battery charge time presented in Montoya et al. (2017) for an electric bus charging in a slow charger. Parameters p^{start} and p^{end} were set to 0 and 1140 min, respectively, to reflect an impossible charge in peak afternoon hours, where electricity is expensive and/or may not be available.

We generated an instance set by setting multiple combinations of values for $|T|$, $|C|$ and $|V_0|$. From the base set of trips, we generated instances having 150, 200 and 250 trips each. For each value of $|T|$, the number of chargers available ($|C|$) was set to 1, 2 and 3, and the number of electric vehicles ($|V_0|$) was set to four different values depending on $\%E \in \{0.25, 0.5, 0.75, 1\}$.

The AVL system used does not report fuel consumption information for diesel buses. Therefore, we consider the total trip time of diesel buses as a proxy to minimize, *i.e.*, $\gamma_j = (t_j^{\text{end}} - t_j^{\text{start}})$ for each $j \in T$.

The data used for the numerical experiments can be accessed at github.com/MatiasAlvo/E-VSP-instances.

4.2. Performance indicators

We defined sets of Key Performance Indicators (KPIs) presented in Tables 3 and 4. Each indicator was classified as a computational performance or solution quality indicator and measured for each instance solved.

Table 4

Set of KPIs measuring solution quality for each instance.

KPI	Definition
gap^{SDP}	Difference of diesel vehicles pulled out between the solution of the sequential dispatch policy and the exact approach
n^D, n^E	Number of diesel and electric vehicles pulled out from the depot, respectively
n	Total number of buses involved in the operation, <i>i.e.</i> , diesel buses pulled out from the depot plus the electric fleet; $n := n^D + V_0 $
t^D, t^E	Total travel time of diesel and electric vehicles, respectively
CT, IT	Total charging and idle time over all chargers, respectively
U	Charger utilization percentage, <i>i.e.</i> , $U := 100 \cdot \frac{CT}{CT+IT}$
\bar{T}^E	Average number of trips served by electric vehicles that were pulled out from the depot

Table 5

Results for instances with 150 trips solved over the first-level objective for the single- and two-stage models.

$ T $	gap^{SDP}	Single-stage model			Two-stage model		
		<360	360–3600	>3600	<360	360–3600	>3600
150	>0	2	0	3	5	0	0
150	0	7	0	0	7	0	0

To compute gap^{SDP} we run a simple sequential dispatch policy (SDP) similar to the one implemented by the public transit operator studied. The solution obtained by the SDP is also used as an initial incumbent solution for both the single- and two-stage formulations. The details of the SDP are described in [Appendix C](#).

4.3. Results on computational performance

We first present computational performance results comparing our two-stage solution to a single-stage benchmark model presented in [Appendix D](#) and based on models proposed by [Rogge et al. \(2018\)](#) and [Wen et al. \(2016\)](#).

[Table 5](#) presents the number of instances with 150 trips optimally solved within different computation time intervals in seconds for the single- and two-stage formulations. We further classify each solution into two subsets, whether the solution provided by the SDP was optimal ($gap^{SDP} = 0$) or not ($gap^{SDP} > 0$).

Empirically, we observe that our two-stage approach optimally solves all small-instances and yields significant solution speed-ups when compared to the single-stage model. Moreover, the single-stage model struggles with three instances and cannot solve them within the 1-h time limit. Some instances are solved by the direct model only because it is initially equipped with an optimal solution provided by the SDP. As the single-stage model is not able to solve instances with $|T| = 150$, further results will only be presented for the two-stage model.

In [Table 6](#) we present our approach's performance for each instance ($|T|, |C|, |V_0|$). For the first-level objective, our approach optimally solves each instance with up to 150 trips within 6 min. Also, it solves all but one instances with 200 trips within 15 min. Finally, all but one instances with 250 trips are solved within 27 min. For the second-level objective, our approach cannot optimally solve almost any instance within 60 min, but reaches relatively small percentage gaps for almost all of the instances with 150 trips. The percentage gap value gets larger for instances with 200 and 250 trips.

As expected, average solution times for the first-level objective and percentage gaps for the second level one significantly increase as a function of the number of trips. The impact of $|V_0|$ in solution times is unclear; replacing diesel vehicles with electric ones adds more variables, but also reduces the number of feasible routes to search for each vehicle. The impact of the number of available chargers in solution performance is unclear; adding more chargers increases the number of variables and constraints, but may deactivate parallel charging capacity constraints making the problem easier to be solved.

No cuts were injected when solving the first-level objective, and they were added in relatively few instances when solving the second-level one. This empirically tells us that the first-stage model is a good approximation of the single-stage one, especially when the first-level objective is set. Notably, no cuts were injected for many instances with solutions having relatively high charger utilization; this result is further explained in [Section 4.4](#). Finally, we observe that in most instances, the time spent solving the second-stage model represents a relatively small fraction of total solution time.

[Table 7](#) details the overall optimality gap and number of cuts injected to the first-stage domain for each objective and whether or not relaxed charging infrastructure capacity constraints [\(3.2m\)](#) are included in the first-stage model. To compare second-level objective results over different cut settings, both versions were solved for a common optimal solution to the first-level objective model. From these results, it becomes clear that constraints [\(3.2m\)](#) do produce a significant improvement in solution performance. Without these constraints, three instances are left unsolved for the first-level objective and gaps significantly increase for the second-level objective. Intuitively, gaps are larger for instances in which the charging infrastructure is relatively more congested, *i.e.*, shared over a larger number of electric buses. Frequently, in such cases the capacity of charging stations becomes binding.

Table 6

Computational performance metrics for each instance.

T	C	V ₀	First-level objective							Second-level objective					
			time ₁	n ^D	gap ₁	gap ^{SDP}	sT ₁	sN ₁	sI ₁	time ₂	t ^D	gap ₂ [%]	sT ₂	sN ₂	sI ₂
150	1	8	12.8	21	0	0	0.6	1	0	>3600.0	12,846	2.6	31.8	142	105
150	1	15	65.6	14	0	1	1.0	2	0	403.3	11,936	0.0	203.6	6	0
150	1	22	55.0	12	0	9	2.1	2	0	>3600.0	11,899	0.3	31.0	16	0
150	1	29	76.2	12	0	12	10.1	3	0	>3600.0	11,700	0.1	24.5	22	0
150	2	8	35.4	21	0	0	0.6	1	0	>3600.0	12,664	1.9	11.8	32	2
150	2	15	36.4	14	0	0	0.7	1	0	>3600.0	6,142	4.5	15.8	20	0
150	2	22	39.3	7	0	0	1.1	1	0	>3600.0	3,488	2.6	2627.1	9	0
150	2	29	328.0	4	0	10	16.9	3	0	2,168.0	3,233	0.0	665.9	5	0
150	3	8	67.9	21	0	0	0.7	1	0	>3600.0	12,657	1.9	12.0	42	16
150	3	15	75.8	14	0	0	0.8	1	0	>3600.0	6,154	5.5	10.5	20	4
150	3	22	71.0	7	0	0	1.3	1	0	>3600.0	1,636	14.9	16.2	13	2
150	3	29	3.7	0	0	1	2.5	1	0	0.0	0	0.0	0.0	0	0
200	1	9	48.4	27	0	0	0.8	1	0	>3600.0	18,751	1.6	52.2	43	27
200	1	18	272.2	18	0	4	3.0	3	0	163.0	18,360	0.0	6.0	5	0
200	1	27	158.4	17	0	8	2.6	2	0	>3600.0	18,218	0.2	7.3	5	0
200	1	36	169.8	17	0	16	12.5	2	0	>3600.0	18,065	0.2	9.7	10	0
200	2	9	120.2	27	0	0	0.9	1	0	>3600.0	17,773	1.0	14.7	27	1
200	2	18	132.1	18	0	0	1.1	1	0	>3600.0	10,642	8.7	96.0	8	2
200	2	27	885.6	9	0	10	10.1	2	0	>3600.0	9,612	0.2	45.4	4	0
200	2	36	807.8	9	0	17	21.4	3	0	>3600.0	9,299	0.1	100.2	6	0
200	3	9	242.5	27	0	0	1.0	1	0	>3600.0	17,695	0.6	11.7	20	1
200	3	18	260.7	18	0	0	1.2	1	0	>3600.0	9,473	10.0	8.9	6	0
200	3	27	275.4	9	0	0	1.8	1	0	>3600.0	7,055	76.3	8.9	5	0
200	3	36	>3600.0	3	1	≥ 7	16.0	3	0	>3600.0	1,089	1.7	853.1	4	0
250	1	15	128.6	42	0	0	1.2	1	0	>3600.0	25,703	0.5	3285.1	4	0
250	1	29	430.5	28	0	10	1.9	2	0	>3600.0	25,664	0.1	35.4	19	0
250	1	43	246.0	26	0	16	2.8	2	0	283.9	25,469	0.0	5.1	5	0
250	1	57	238.3	26	0	24	7.3	2	0	1,453.6	25,352	0.0	6.0	6	0
250	2	15	366.1	42	0	0	1.3	1	0	>3600.0	20,395	6.9	14.6	14	1
250	2	29	349.5	28	0	0	1.3	1	0	>3600.0	16,613	0.2	1585.9	4	0
250	2	43	1588.2	16	0	13	6.2	2	0	>3600.0	16,896	0.1	1037.8	5	0
250	2	57	1513.6	16	0	27	29.8	2	0	>3600.0	16,648	0.1	876.4	4	0
250	3	15	729.0	42	0	0	1.4	1	0	>3600.0	21,446	12.0	8.7	11	1
250	3	29	730.8	28	0	0	1.5	1	0	>3600.0	26,272	67.9	2.4	3	0
250	3	43	752.2	14	0	0	2.2	1	0	>3600.0	15,669	48.0	4.1	3	0
250	3	57	>3600.0	32	24	≥ 0	45.5	1	0	>3600.0	7,921	0.3	120.4	2	0

Table 7

Computational performance metrics for each instance with 150 trips, with and without including relaxed charging infrastructure capacity constraints in the first-stage model.

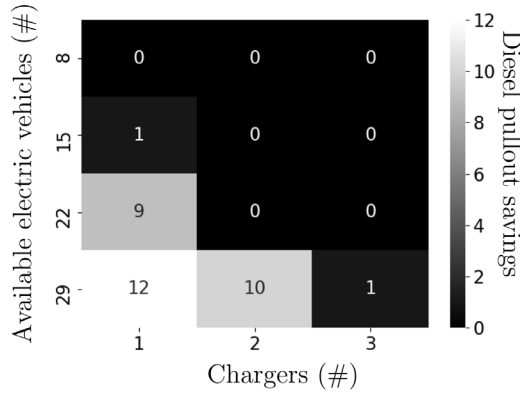
T	C	V ₀	With first-stage capacity constraints				Without first-stage capacity constraints			
			gap_1	sI_1	$gap_2^{\%}$	sI_2	gap_1	sI_1	$gap_2^{\%}$	sI_2
150	1	8	0	0	2.6	105	0	0	6.2	672
150	1	15	0	0	0.0	0	0	5	53.2	1559
150	1	22	0	0	0.3	0	8	13,375	86.6	1250
150	1	29	0	0	0.1	0	19	8,459	89.7	9906
150	2	8	0	0	1.9	2	0	0	1.2	262
150	2	15	0	0	4.5	0	0	0	3.8	137
150	2	22	0	0	2.6	0	0	0	63.3	1296
150	2	29	0	0	0.0	0	5	3,830	89.7	4148
150	3	8	0	0	1.9	16	0	0	1.3	147
150	3	15	0	0	5.5	4	0	0	2.8	8
150	3	22	0	0	14.9	2	0	0	7.2	25
150	3	29	0	0	0.0	0	0	0	0.0	0

4.4. Results on solution structure and performance

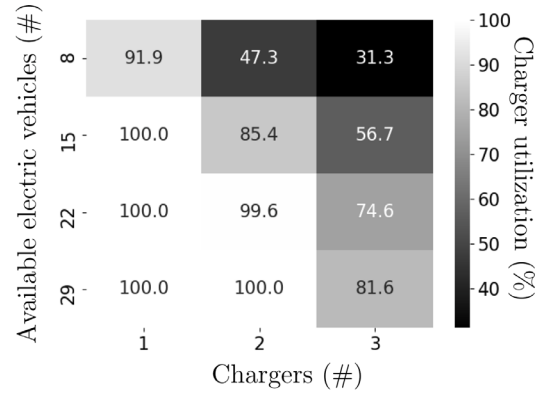
We now present results related to our solution's structure and quality. To do so, we consider all previous instances with 150 trips and empirically study the optimal solution structure and objective value as a function of instance settings, such as the number of available chargers and the relative size of the electric fleet. All instances with 150 trips can be covered by exactly 29 diesel

Table 8
Operational metrics for instances with 150 trips.

$ C $	$ V_0 $	n^E	n^D	n^V	gap^{SDP}	t^E	t^D	CT	IT	U	\bar{T}^E
1	8	8	21	29	0	8,087	12,846	1048	92	91.9	7.4
1	15	15	14	29	1	8,997	11,936	1140	0	100.0	4.1
1	22	18	12	34	9	9,034	11,899	1140	0	100.0	2.8
1	29	18	12	41	12	9,233	11,700	1140	0	100.0	2.2
2	8	8	21	29	0	8,269	12,664	1078	1202	47.3	7.5
2	15	15	14	29	0	14,791	6,142	1947	333	85.4	7.1
2	22	22	7	29	0	17,445	3,488	2272	8	99.6	5.6
2	29	25	4	33	10	17,700	3,233	2280	0	100.0	4.3
3	8	8	21	29	0	8,276	12,657	1069	2351	31.3	7.5
3	15	15	14	29	0	14,779	6,154	1940	1480	56.7	7.1
3	22	22	7	29	0	19,297	1,636	2553	867	74.6	6.3
3	29	29	0	29	1	20,933	0	2789	631	81.6	5.2



(a) Difference of diesel bus pullouts between the SDP and the exact solution.



(b) Charger utilization (%) in the exact solution.

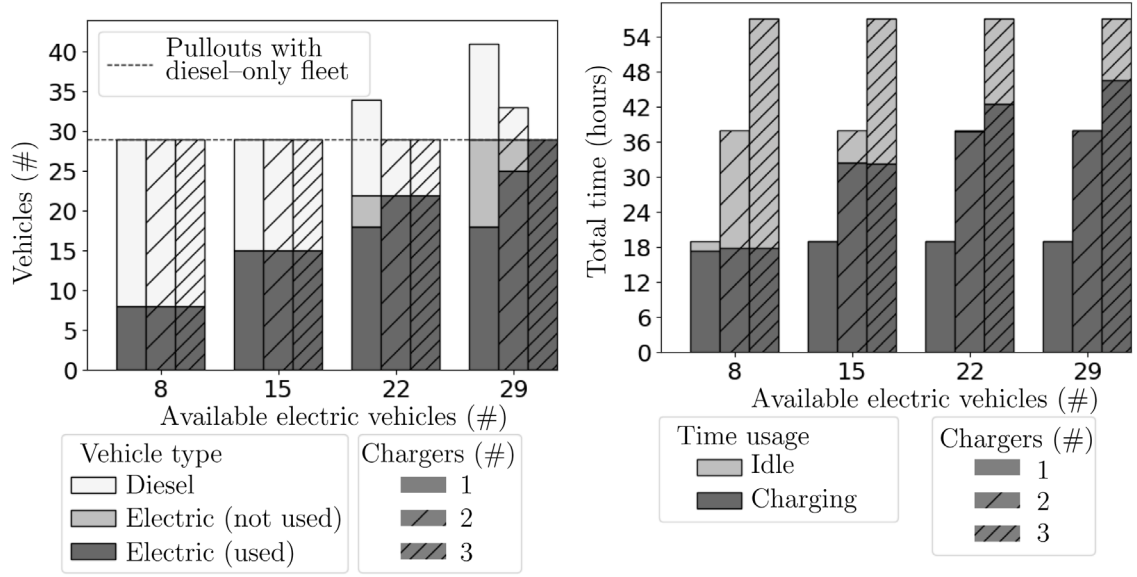
Fig. 6. Solution quality KPIs for different settings of available electric vehicles and chargers. Instances with 150 trips.

vehicles if no electric bus is available. Table 8 presents results for each instance solved. Empirically, we see how the number of available electric buses and chargers can significantly impact bus utilization. For all instances, the total number of buses involved in the operation (n) is no smaller than 29 and reaches up to 41 in a highly constrained instance in which 29 electric buses share one charger. In this case, 11 electric buses are left unused. Conversely, all instances with 3 chargers use 29 buses, meaning that imposing an electric fleet does not increase the number of buses involved. We conclude that the number of additional diesel buses required to complement the electric fleet in trip coverage is relatively higher for a highly congested charging infrastructure.

In Table 8, we also see that, for a fixed number of chargers ($|C|$), the average number of trips executed by an electric vehicle pulled out from the depot (\bar{T}^E) reduces as a function of the electric fleet size ($|V_0|$). This suggests that, when there exists a relatively large number of electric buses over the number of available chargers, electric buses are prevented from being further utilized. Furthermore, there is higher charger utilization (large values of U) in instances with a larger ratio of electric vehicles over available chargers and, consequently, low values of \bar{T}^E . As we observe in Table 6, fewer cuts are injected in these instances. This may be counter-intuitive and may be explained due to the additional flexibility available to find a feasible charging schedule in the second-stage model, which probably makes the injection of cuts less likely.

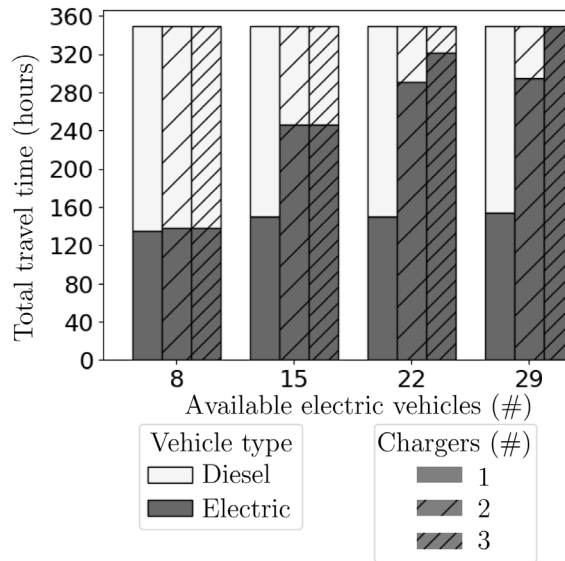
Fig. 6a presents the difference in diesel buses used between the SDP and exact solutions over different settings of available electric vehicles and chargers. Fig. 6b presents the charger utilization percentage over the same settings. As noticed, the difference in diesel buses pulled out from the depot is one or zero for less congested charging infrastructures; this number increases as chargers become utilized closer to their capacity. We conclude that the advantage of our approach over the simpler SDP is larger when the charging infrastructure is more congested.

Fig. 7a presents the total number of buses involved in each solution (n) as a function of the available electric fleet size ($|V_0|$) and number of available chargers ($|C|$). Fig. 7b details the total charging (CT) and idle time (IT) of all chargers at the depot for each value of $|C|$ and $|V_0|$. Combined, both figures empirically suggest that the number of required buses directly depends on the charger congestion effects produced by both $|C|$ and $|V_0|$. For example, consider the instance with 29 electric vehicles and 1 charger. We



(a) Number of electric and diesel buses used.

(b) Total charger utilization



(c) Travel time executed by electric and diesel buses.

Fig. 7. Solution quality KPIs for each setting of $|V_0|$ and $|C|$. Instances with 150 trips.

can reduce n from 41 to 29 if we add two more chargers or if we replace 14 electric vehicles with two diesel ones. Nonetheless, the potential reduction in n is 0 if 3 chargers are already available. The value of an additional charger is also zero when the available number of electric buses is 15 and only one charger is available. This suggests managers to measure congestion of the charging infrastructure to correctly assess the value of an additional charger and electric bus before making investment decisions.

Regarding the secondary objective, Fig. 7c presents the total travel times of electric (t^E) and diesel (t^D) buses as a function of parameters $|V_0|$ and $|C|$. We empirically observe that the marginal reduction in t^D produced by adding a new charger is relatively higher in relatively more congested instances (with more electric buses). Also, the marginal reduction in t^D provided by an additional electric vehicle is relatively higher in less congested instances (with more chargers).

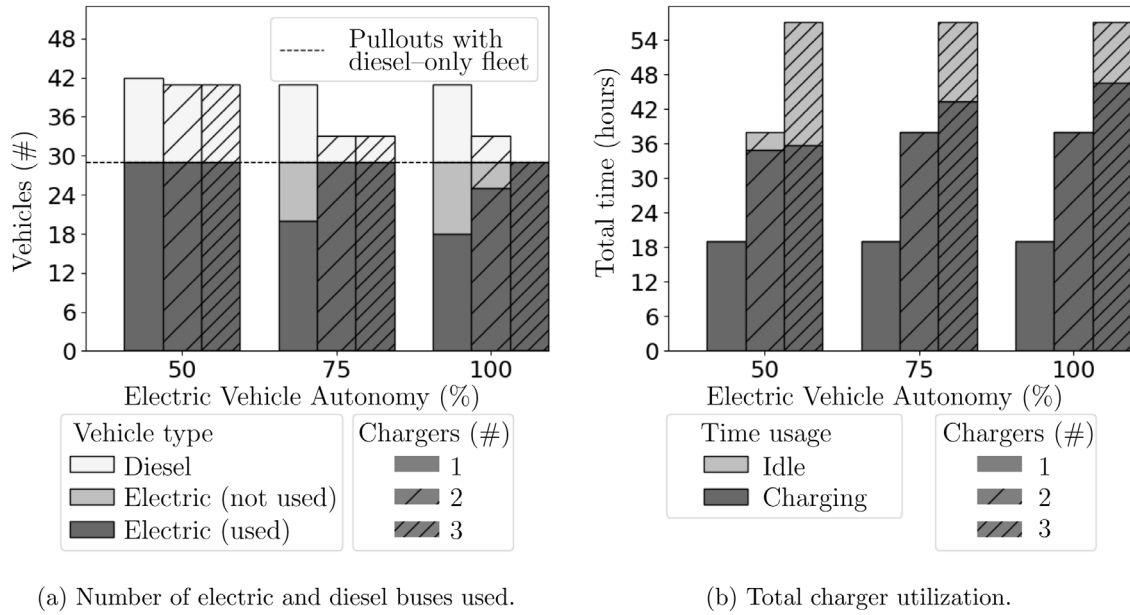


Fig. 8. Solution quality KPIs for different electric vehicle autonomies and number of chargers. Instances with 150 trips and a fleet of 29 electric vehicles.

4.5. Sensitivity analysis on battery capacity

In this subsection, we further analyze the impact of reduced electric vehicle autonomy in solution quality. Electric vehicle autonomy is represented in parameter $EVA \in \{50\%, 75\%, 100\%\}$ as the relative size of the battery compared to the one in used in the base case experiment. It may represent scenarios such as operating with deteriorated batteries or investing in cheaper battery alternatives. Fig. 8a presents the number of buses involved (n) for an instance with 29 electric buses and different values of $|C|$ and EVA . Fig. 8b details the total charging time (CT) and charger idle time (IT) over the same cases. Empirically, these figures show how a reduced autonomy directly impacts on solution performance and charger congestion. The number of diesel buses used increases as EVA is smaller, especially if more chargers are available. Instances with fewer chargers are less impacted with an EVA reduction, probably because they are already congested and rest their operation relatively more on diesel vehicles.

For example, consider the instance with 1 charger. A 50% reduction in autonomy barely increases n . As the chargers are congested, the electric fleet is already struggling, underutilized and more diesel vehicles are operating. On the other hand, for the instance with 2 chargers a 50% autonomy reduction significantly increases n . Probably, because it changes from a low congested setting to a high congested one. A reduced battery autonomy may also impact the performance of the electric fleet during peak hours (see Fig. 5a). This behavior can be seen for a particular instance having 2 chargers and 29 electric buses available in Fig. 9a and 9b.

5. Conclusions

We engage in solving a single-depot electric bus dispatch problem with limited parallel charging capacity and partial charging tasks.

As a single-stage formulation yields an intractable model for medium-sized instances, we propose an exact two-stage Benders' type decomposition, solved with a framework inspired by Codato and Fischetti (2006). In this approach, the solution of the first-stage model identifies a feasible trip schedule for each bus in a formulation that relaxes the sequencing of charging tasks in each charger. The overall feasibility of this set of trip schedules is later tested in a second-stage problem which attempts to identify a complementary and feasible pair of battery charge and charger schedules. If no such pair exists, then feasibility cuts are injected into the first-stage model to ban such first-stage solution.

As shown by numerical results, the proposed solution method outperforms the single-stage model in terms of computational times. Also, it outperforms a simple sequential dispatch policy in terms of solution quality, especially when charger utilization is relatively high.

We also empirically assess the marginal benefits provided by an additional charger or an electric bus. Empirically, we suggest decision makers to invest in additional chargers if relatively more electric buses per charger are available. Also, the additional value of an electric vehicle is relatively higher in fleets having relatively less electric vehicles. For instance, if two bus terminals are managed by a single operator, then it may be convenient to set two mixed fleet operations in contrast to one fully electric and another fully diesel bus operation.

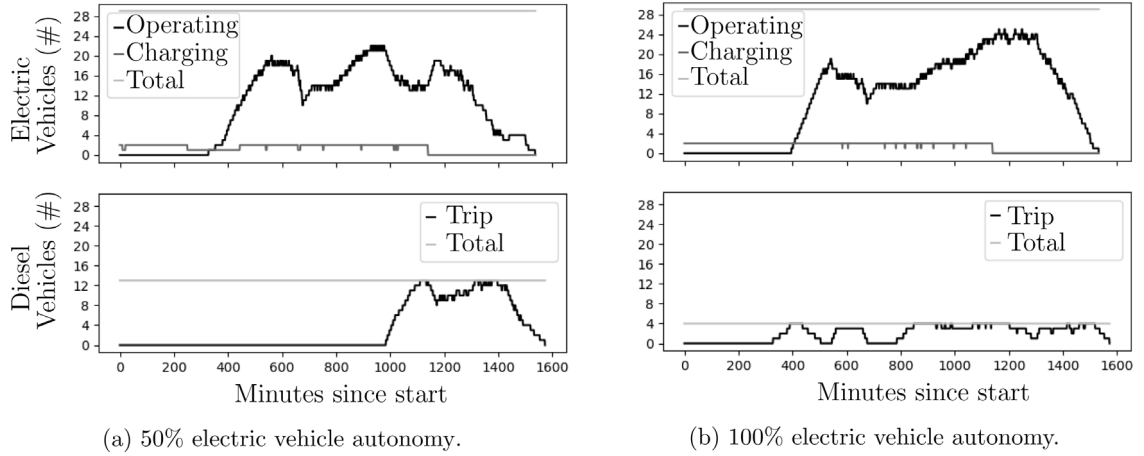


Fig. 9. Status of the electric and diesel fleet per minute. Instances with 150 trips, 2 chargers and 29 electric vehicles available.

Table 9

Definition of the decision variables used in our first-stage model.

Variable	Definition
$x_a^\ell \in \{0, 1\}$	Indicates whether or not a bus of type ℓ traverses arc $a \in A_\ell$
$e_a \geq 0$	Represents the battery's SoC level immediately after a possible battery charge in between nodes u and v if $a = (u, v) \in \bar{A}_0$ or the remaining SoC in the bus battery immediately after leaving node u if $a = (u, v) \notin \bar{A}_0$
$y_a^c \in \{0, 1\}$	Indicates whether or not a charge occurs at charger $c \in C$ for an electric vehicle traversing arc $a \in \bar{A}_0$
$g_a^c \geq 0$	Represents the SoC level injected to the battery at charger $c \in C$ for an electric vehicle traversing arc $a \in \bar{A}_0$

Lastly, we observe in our experiments that a reduction in electric bus autonomy has more impact in instances with less congested chargers relying more on the electric fleet.

The problem and methodology presented can be further extended in several directions. First, we could model non-linear SoC charging rates as a function of charge time. A first approach would be to implement a piecewise linear relation to keep the model's linear structure. We could also study a robust and/or dynamic decision planning model to represent a more realistic bus dispatch operation over trips having stochastic travel time and energy consumption. Finally, a multi-depot problem could be studied considering multiple bus services interacting within a public transit network.

CRediT authorship contribution statement

Matías Alvo: Conceptualization, Methodology, Software, Validation, Investigation, Writing – original draft, Visualization, Writing – reviewing and editing. **Gustavo Angulo:** Conceptualization, Methodology, Supervision, Investigation, Writing – reviewing and editing. **Mathias A. Klapp:** Conceptualization, Methodology, Supervision, Investigation, Writing – reviewing and editing.

Acknowledgments

Mathias Klapp thanks ANID (Agencia Nacional de Investigación y Desarrollo), Chile, for its support through the FONDECYT Iniciación Project number 11190392.

All authors would like to thank TrackTec S.A. for generously providing data for this work.

Funding

Mathias Klapp thanks ANID (Agencia Nacional de Investigación y Desarrollo), Chile, for its support through the FONDECYT Iniciación Project number 11190392.

Appendix A. List of variables used in the two-stage formulation

See Tables 9 and 10.

Table 10

Definition of the decision variables used in our second-stage model.

Variable	Definition
$v_{i,d} \geq 0$	Represents the SoC level charged for the d th possible charge of bus i for each $(i,d) \in \Omega$
$b_{i,d} \geq 0$	Represents the start time for the d th possible charge of bus i for each $(i,d) \in \Omega$
$z_a \in \{0, 1\}$	Encodes charger assignment and sequencing. In particular, for $a = ((i_1, d_1), (i_2, d_2)) \in \Gamma$, variable $z_{(i_1, d_1), (i_2, d_2)}$ represents whether possible charging tasks (i_1, d_1) and (i_2, d_2) are consecutively executed in one charger
$\eta \geq 0$	Represents the maximum violation over all constraints in (3.4a)

Appendix B. Proof of Proposition 1

Let $q, q' \in \Omega$ with $\hat{\alpha}_q \leq \hat{\alpha}_{q'}$ and $\hat{\beta}_q \leq \hat{\beta}_{q'}$ such that, in a solution to the second-stage problem, $z_{(q',q)} = 1$. We will demonstrate that we can find a solution such that $z_{(q',q)} = 0$ with the same objective value. Current variable values will be denoted with a 0 super-index and newly assigned values with a 1 super-index. Let p and s be the nodes that fulfill $z_{(p,q')}^0 = 1$ and $z_{(q,s)}^0 = 1$ and assume without loss of generality that $(q', s) \in \Gamma$ and $(p, q) \in \Gamma$. Trivially, current variable values fulfill $\hat{\alpha}_q \leq \hat{\alpha}_{q'} \leq b_{q'}^0 \leq b_{q'}^0 + v_{q'}^0 \leq b_q^0 \leq b_q^0 + v_q^0 \leq \hat{\beta}_q \leq \hat{\beta}_{q'}$. Then, we can interchange nodes q and q' by setting $z_{(p,q')}^1 = z_{(p,q)}^1 = z_{(q,s)}^1 = 0$, $z_{(p,q)}^1 = z_{(q,q')}^1 = z_{(q',s)}^1 = 1$ and updating charge start times as $b_q^1 = b_{q'}^0$ and $b_{q'}^1 = b_{q'}^0 + v_{q'}^0$, while maintaining charge durations and, therefore, the current objective value. As $\hat{\alpha}_q \leq b_{q'}^0 = b_q^1$ and $b_q^1 + v_q^1 = b_{q'}^0 + v_{q'}^0 + v_q^0 \leq b_{q'}^0 + v_{q'}^0 \leq b_q^0 + v_q^0 \leq \hat{\beta}_{q'}$, this yields feasible variable values for q and q' , leaving other charging events unchanged.

Appendix C. Sequential dispatch policy

We assume that, based on experience, the dispatcher knows the values of \bar{d}^{\max} and, therefore, a lower bound for n^D . As she knows that at least $(\bar{d}^{\max} - |V_0|)$ diesel vehicles are going to be used, the dispatcher prioritizes them (and every diesel vehicle already used) over electric vehicles when dispatching. Dispatches are assumed to be done sequentially by trip start time, using the following prioritization system over vehicles currently at the depot: (1) Diesel vehicle already used or prioritized; (2) Electric vehicle waiting at the depot for the longest time; (3) Diesel vehicle not used or prioritized. Furthermore, if an electric vehicle has time to be charged before its next assigned trip, it will charge as long as possible, and in the charger that was vacated earliest.

Appendix D. Single-stage formulation

In this section we present a single-stage MIP model which is partly based on the models defined by Wen et al. (2016) and Rogge et al. (2018). The problem is represented in a digraph that models trip and battery charge schedules, and a second digraph that plans charger schedules.

Sets V_0, V_1, V, T, C, L , sink 0 and parameters $f, p^{\text{start}}, p^{\text{end}}, \bar{e}^{\min}, \bar{e}^{\max}, \bar{e}^{\text{end}}, \bar{e}_i, \bar{e}_j, t_j^{\text{start}}$ and t_j^{end} are defined as in Section 3.

We are going to make two charger copies (equivalently, possible charging tasks) for each trip $j \in T$. The first copy (denoted as p copy) represents a charge happening directly from the source and immediately preceding trip j . The second copy (denoted as r copy) represents a charge happening directly after serving trip j . Charger copy $n := (q, j)$ for $q \in \{p, r\}$ and $j \in T$ defines a time interval $[\alpha_n, \beta_n]$ when an electric bus visiting it may charge. Accordingly, α_n is set to p^{start} if $q = p$ and to $\max(p^{\text{start}}, t_j^{\text{end}})$ if $q = r$, while β_n is set to $\min(p^{\text{end}}, t_j^{\text{start}})$ if $q = p$ and to p^{end} if $q = r$. Let sets $P = \{(p, j) : j \in T, \alpha_{(p,j)} < \beta_{(p,j)}\}$ and $R = \{(r, j) : j \in T, \alpha_{(r,j)} < \beta_{(r,j)}\}$ be the sets containing p -type and r -type charger copies, respectively, for which it is feasible for a charge to occur. Then, let $F = P \cup R$ be a set containing all such charger copies.

We encode trip and battery charge itineraries in a digraph $G = (N, A)$, where the set of nodes $N := T \cup V \cup F \cup \{0\}$ is formed by all trips, a source for each electric bus, one source node for all diesel buses, all charger copies, and a sink, respectively.

Set A contains feasible arcs (u, v) connecting nodes $u, v \in N$. Arcs are considered feasible according to the following rules: (1) An arc exists from each vehicle node $i \in V$ to each trip $j \in T$ and from each trip j to the sink; (2) An arc exists from trip $j_1 \in T$ to trip $j_2 \in T$ if and only if $t_{j_1}^{\text{end}} \leq t_{j_2}^{\text{start}}$; (3) For charger copy $(p, j_1) \in P$, the only possible arcs are from vehicle nodes to the charger copy, and from the charger copy to trip j_1 ; (4) For charger copy $(r, j_1) \in R$, the only possible arcs are from trip j_1 to the charger copy, or from the charger copy to the sink or to a trip j_2 such that $t_{j_1}^{\text{end}} \leq t_{j_2}^{\text{start}}$.

Then, define sets $A_0 := \{(u, v) \in A : u \in T \cup V_0 \cup F\}$ and $A_1 := \{(u, v) \in A : u \in T \cup V_1, v \notin F\}$ as the subset of arcs that electric and diesel buses can use, respectively. Also, define the set of arcs in A_ℓ leaving and entering node $i \in N$ as $\delta_\ell^+(i) := \{(i, j) \in A_\ell : j \in N\}$ and $\delta_\ell^-(i) := \{(j, i) \in A_\ell : j \in N\}$, respectively.

Charging station itineraries are encoded in a digraph $H = (D, B)$, where the set of nodes $D := \{\underline{S}\} \cup F \cup \{\bar{S}\}$ is formed by all charger copies, a source \underline{S} , and a sink \bar{S} , respectively. Set B contains arcs (u, v) connecting time-feasible nodes $u, v \in D$, which models sequencing decisions. Let $\alpha_{\underline{S}} = \beta_{\underline{S}} = p^{\text{start}}$ and $\alpha_{\bar{S}} = \beta_{\bar{S}} = p^{\text{end}}$. So, $B = \{(u, v) : u \in \{\underline{S}\} \cup F, v \in F \cup \{\bar{S}\}, \alpha_u < \beta_v\}$. Then, define the set of arcs in B leaving and entering node $i \in D$ as $\Delta^+(i) := \{(i, j) \in B : j \in D\}$ and $\Delta^-(i) := \{(j, i) \in B : j \in D\}$, respectively.

Provided the above information, we are now ready to define all decision variables. Let $x_a^\ell \in \{0, 1\}$ be a binary variable defined for each $\ell \in L$ and $a \in A_\ell$ representing a vehicle of type ℓ traversing arc a . Decision vector \mathbf{x} is used to encode a set of at most $|V_0| + \bar{d}^{\max}$ bus itineraries as paths from each node $i \in V$ to node 0 visiting each trip node in T exactly once.

For each electric bus arc $a = (u, v) \in A_0$, we also define a continuous variable $e_a \geq 0$ representing the battery's SoC just after leaving node $u \in N$. So, decision vector \mathbf{e} encodes battery SoC levels for electric buses. Also, we set a binary variable w_a for each

arc $a \in B$, representing that two possible charging tasks are served by the same charger in consecutive order. Finally, we define continuous variables $b_j \geq 0$ and $t_j \geq 0$ representing the charged amount and start time, respectively, for the only possible charge in charger copy $j \in F$. Therefore, decision vectors \mathbf{w} , \mathbf{b} and \mathbf{t} encode charger itineraries. For trips $j_1, j_2 \in T$, we define big-M parameters $M_{j_1 j_2} = \beta_{j_1} - \alpha_{j_2}$, which are upper bounds for $(b_{j_1} + t_{j_1}) - b_{j_2}$.

Objective function

The objective function is equivalent to the one defined in Section 3.

$$\min \sum_{a \in \delta_1^+(v_1)} x_a^1, \quad (\text{D.1a})$$

$$\min \sum_{a := (u,v) \in A_1 : v \in T} \gamma_v \cdot x_a^1. \quad (\text{D.1b})$$

Feasibility constraints

$$\sum_{\ell \in L} \sum_{a \in \delta_\ell^+(j)} x_a^\ell = 1, \quad \forall j \in T, \quad (\text{D.2a})$$

$$\sum_{a \in \delta_\ell^-(j)} x_a^\ell - \sum_{a \in \delta_\ell^+(j)} x_a^\ell = 0, \quad \forall j \in T \cup F, \ell \in L, \quad (\text{D.2b})$$

$$\sum_{a \in \delta_0^+(j)} x_a^0 \leq 1, \quad \forall j \in V_0, \quad (\text{D.2c})$$

$$\sum_{a \in \delta_1^+(v_1)} x_a^0 \leq \bar{d}^{\max}, \quad (\text{D.2d})$$

$$\sum_{a \in \Delta^-(j)} w_a - \sum_{a \in \Delta^+(j)} w_a = 0, \quad \forall j \in F, \quad (\text{D.2e})$$

$$\sum_{a \in \Delta^+(S)} w_a \leq |C|, \quad (\text{D.2f})$$

$$\sum_{a \in \Delta^+(j)} w_a - \sum_{a \in \delta_0^+(j)} x_a^0 = 0, \quad \forall j \in F, \quad (\text{D.2g})$$

$$\alpha_j \leq b_j, \quad \forall j \in F, \quad (\text{D.2h})$$

$$b_j + t_j \leq \beta_j, \quad \forall j \in F, \quad (\text{D.2i})$$

$$b_{j_1} + t_{j_1} - \alpha_{j_1} \leq \sum_{j_2 \in T : (j_1, j_2) \in A_0} (t_{j_2}^{\text{start}} - \alpha_{j_1}) \cdot x_{(j_1, j_2)}^0, \quad \forall j_1 \in R, \quad (\text{D.2j})$$

$$b_{j_1} + t_{j_1} \leq b_{j_2} + M_a \cdot (1 - w_a), \quad \forall a = (j_1, j_2) \in B, \quad (\text{D.2k})$$

$$\sum_{a \in \delta_0^-(j)} e_a + f \cdot t_j = \sum_{a \in \delta_0^+(j)} e_a, \quad \forall j \in F, \quad (\text{D.2l})$$

$$\sum_{a \in \delta_0^-(j)} e_a - \bar{e}^j \cdot \sum_{a \in \delta_0^+(j)} x_a^0 = \sum_{a \in \delta_0^+(j)} e_a, \quad \forall j \in T, \quad (\text{D.2m})$$

$$e_a = x_a \cdot \bar{e}_i, \quad \forall i \in V_0, a \in \delta_0^+(i), \quad (\text{D.2n})$$

$$\bar{e}^{\min} \cdot x_a^0 \leq e_a, \quad \forall j \in T, a \in \delta_0^+(j), \quad (\text{D.2o})$$

$$\bar{e}^{\text{end}} \cdot x_a^0 \leq e_a, \quad \forall a \in \delta_0^-(\bar{S}), \quad (\text{D.2p})$$

$$e_a \leq \bar{e}^{\max} \cdot x_a^0, \quad \forall a \in A_0, \quad (\text{D.2q})$$

$$x_a^l \in \{0, 1\}, \quad \forall l \in L, a \in A_l, \quad (\text{D.2r})$$

$$w_a \in \{0, 1\}, \quad \forall a \in B, \quad (\text{D.2s})$$

$$e_a \geq 0, \quad \forall a \in A_0, \quad (\text{D.2t})$$

$$b_j \geq 0, \quad \forall j \in F, \quad (\text{D.2u})$$

$$t_j \geq 0, \quad \forall j \in F. \quad (\text{D.2v})$$

Constraints (D.2a) guarantee that all trips are executed by exactly one vehicle. Constraints (D.2b)–(D.2d) enforce vehicle flow conservation constraints for each vehicle starting from node $i \in V$. Constraints (D.2e) and (D.2f) impose flow conservation constraints for nodes in D , while (D.2g) ensures compatibility between digraphs G and H . Constraints (D.2h)–(D.2k) impose time-feasibility constraints for consecutive nodes. Constraints (D.2l)–(D.2n) ensure battery SoC flow conservation for each node. Then, constraints (D.2o)–(D.2q) guarantee that battery SoC is kept within feasible ranges. Finally, constraints (D.2r)–(D.2v) define variable domains.

References

- Adler, J.D., Mirchandani, P.B., 2016. The vehicle scheduling problem for fleets with alternative-fuel vehicles. *Transp. Sci.* 51 (2), 441–456.
- Andelmin, J., Bartolini, E., 2017. An exact algorithm for the green vehicle routing problem. *Transp. Sci.* 51 (4), 1288–1303.
- Andelmin, J., Bartolini, E., 2019. A multi-start local search heuristic for the green vehicle routing problem based on a multigraph reformulation. *Comput. Oper. Res.* 109, 43–63.
- Benders, J.F., 2005. Partitioning procedures for solving mixed-variables programming problems. *Comput. Manag. Sci.* 2 (1), 3–19.
- Bodin, L., Golden, B., Assad, A., Ball, M., 1983. Routing and scheduling of vehicles and crews: the state of the art. *Comput. Oper. Res.* 10, 62–212.
- Bruglieri, M., Mancini, S., Pezzella, F., Pisacane, O., 2019a. A path-based solution approach for the green vehicle routing problem. *Comput. Oper. Res.* 103, 109–122.
- Bruglieri, M., Mancini, S., Pisacane, O., 2019b. The green vehicle routing problem with capacitated alternative fuel stations. *Comput. Oper. Res.* 112, 104759.
- Bunte, S., Kliewer, N., 2009. An overview on vehicle scheduling models. *Public Transp.* 1 (4), 299–317.
- Codato, G., Fischetti, M., 2006. Combinatorial Benders' cuts for mixed-integer linear programming. *Oper. Res.* 54 (4), 756–766.
- Desaulniers, G., Errico, F., Irnich, S., Schneider, M., 2016. Exact algorithms for electric vehicle-routing problems with time windows. *Oper. Res.* 64 (6), 1388–1405.
- Desaulniers, G., Lavigne, J., Soumis, F., 1998. Multi-depot vehicle scheduling problems with time windows and waiting costs. *European J. Oper. Res.* 111 (3), 479–494.
- Desrosiers, J., Dumas, Y., Solomon, M.M., Soumis, F., 1995. Time constrained routing and scheduling. *Handbooks Oper. Res. Management Sci.* 8, 35–139.
- Drexel, M., 2012. Synchronization in vehicle routing—a survey of VRPs with multiple synchronization constraints. *Transp. Sci.* 46 (3), 297–316.
- Erdoğan, S., Miller-Hooks, E., 2012. A green vehicle routing problem. *Transp. Res. E* 48 (1), 100–114.
- Etezadi-Amoli, M., Choma, K., Stefani, J., 2010. Rapid-charge electric-vehicle stations. *IEEE Trans. Power Deliv.* 25 (3), 1883–1887.
- Felipe, A., Ortuño, M.T., Righini, G., Tirado, G., 2014. A heuristic approach for the green vehicle routing problem with multiple technologies and partial recharges. *Transp. Res. E* 71, 111–128.
- Foulkes, J.D., Prager, W., Warner, W.H., 1954. On bus schedules. *Manage. Sci.* 1 (1), 41–48.
- Freling, R., Paixão, J.M., 1995. Vehicle scheduling with time constraint. In: *Computer-Aided Transit Scheduling*. Springer, pp. 130–144.
- Froger, A., Mendoza, J.E., Jabali, O., Laporte, G., 2019. Improved formulations and algorithmic components for the electric vehicle routing problem with nonlinear charging functions. *Comput. Oper. Res.* 104, 256–294.
- Froger, A., Mendoza, J.E., Jabali, O., Laporte, G., 2021. The electric vehicle routing problem with capacitated charging stations. *hal-02386167v2*.
- Goeke, D., Schneider, M., 2015. Routing a mixed fleet of electric and conventional vehicles. *European J. Oper. Res.* 245 (1), 81–99.
- Guo, Congcong, Wang, Chunlu, Zuo, Xingquan, 2019. A genetic algorithm based column generation method for multi-depot electric bus vehicle scheduling. In: *Proceedings of the Genetic and Evolutionary Computation Conference Companion*. pp. 367–368.
- Heid, B., Hensley, R., Knupfer, S., Tschiesner, A., 2017. What's sparking electric vehicle adoption in the truck industry?.
- Hiermann, G., Puchinger, J., Ropke, S., Hartl, R.F., 2016. The electric fleet size and mix vehicle routing problem with time windows and recharging stations. *European J. Oper. Res.* 252 (3), 995–1018.
- Keskin, M., Catay, B., 2018. A matheuristic method for the electric vehicle routing problem with time windows and fast chargers. *Comput. Oper. Res.* 100, 172–188.
- Koç, Ç., Jabali, O., Mendoza, J.E., Laporte, G., 2019. The electric vehicle routing problem with shared charging stations. *Int. Trans. Oper. Res.* 26 (4), 1211–1243.
- Koç, Ç., Karaoglan, I., 2016. The green vehicle routing problem: A heuristic based exact solution approach. *Appl. Soft Comput.* 39, 154–164.
- Kunith, A., Mendelevitch, R., Goehlich, D., 2017. Electrification of a city bus network—An optimization model for cost-effective placing of charging infrastructure and battery sizing of fast-charging electric bus systems. *Int. J. Sustain. Transp.* 11 (10), 707–720.
- Lee, C., 2020. An exact algorithm for the electric-vehicle routing problem with nonlinear charging time. *J. Oper. Res. Soc.* 1–24.
- Li, J.Q., 2014. Transit bus scheduling with limited energy. *Transp. Sci.* 48 (4), 521–539.
- Li, L., Lo, H.K., Xiao, F., 2019. Mixed bus fleet scheduling under range and refueling constraints. *Transp. Res. C* 104, 443–462.
- Margolis, J., 2019. China dominates the electric bus market, but the US is getting on board.
- Millner, A., 2010. Modeling lithium ion battery degradation in electric vehicles. In: *2010 IEEE Conference on Innovative Technologies for an Efficient and Reliable Electricity Supply*. IEEE, pp. 349–356.
- Montoya, A., Guéret, C., Mendoza, J.E., Villegas, J.G., 2016. A multi-space sampling heuristic for the green vehicle routing problem. *Transp. Res. C* 70, 113–128.
- Montoya, A., Guéret, C., Mendoza, J.E., Villegas, J.G., 2017. The electric vehicle routing problem with nonlinear charging function. *Transp. Res. B* 103, 87–110.
- Organisation for Economic Cooperation and Development (OECD), 2016. *The Economic Consequences of Outdoor Air Pollution*. OECD Publishing, Paris.
- Pelletier, S., Jabali, O., Laporte, G., 2016. 50Th anniversary invited article—goods distribution with electric vehicles: review and research perspectives. *Transp. Sci.* 50 (1), 3–22.
- Perumal, S., Dollevoet, T., Huisman, D., Lusby, R., Larsen, J., Riis, M., 2020. Solution approaches for integrated vehicle and crew scheduling with electric buses. *Comput. Oper. Res.* 132, 105268.
- Pollet, B.G., Staffell, I., Shang, J.L., 2012. Current status of hybrid, battery and fuel cell electric vehicles: From electrochemistry to market prospects. *Electrochim. Acta* 84, 235–249.
- Quarles, N., Kockelman, K.M., Mohamed, M., 2020. Costs and benefits of electrifying and automating bus transit fleets. *Sustainability* 12 (10), 3977.
- Rahmanian, R., Crainic, T.G., Gendreau, M., Rei, W., 2017. The Benders decomposition algorithm: A literature review. *European J. Oper. Res.* 259 (3), 801–817.
- Rinaldi, M., Parisi, F., Laskaris, G., D'Ariano, A., Viti, F., 2018. Optimal dispatching of electric and hybrid buses subject to scheduling and charging constraints. In: *2018 21st International Conference on Intelligent Transportation Systems (ITSC)*. IEEE, pp. 41–46.
- Rogge, M., van der Hurk, E., Larsen, A., Sauer, D.U., 2018. Electric bus fleet size and mix problem with optimization of charging infrastructure. *Appl. Energy* 211, 282–295.
- Sassi, O., Oulamara, A., 2016. Electric vehicle scheduling and optimal charging problem: complexity, exact and heuristic approaches. *Int. J. Prod. Res.* 55 (2), 519–535.
- Schneider, M., Stenger, A., Goeke, D., 2014. The electric vehicle-routing problem with time windows and recharging stations. *Transp. Sci.* 48 (4), 500–520.
- Scriven, R., 2019. LATAM electric bus market strong but may fail to reach potential.
- Sokhi, R., 2011. *World Atlas of Atmospheric Pollution*. Anthem Press.
- Tang, X., Lin, X., He, F., 2019. Robust scheduling strategies of electric buses under stochastic traffic conditions. *Transp. Res. C* 105, 163–182.
- Union Internationale des Transports Publics (UITP), 2019. *The Impact of Electric Buses on Urban Life*. Union Internationale des Transports Publics.
- van Kooten Niekerk, M.E., van den Akker, J.M., Hoogeveen, J.A., 2017. Scheduling electric vehicles. *Public Transp.* 9 (1), 155–176.
- Wang, Y., Huang, Y., Xu, J., Barclay, N., 2017. Optimal recharging scheduling for urban electric buses: A case study in Davis. *Transp. Res. E* 100, 115–132.
- Wen, M., Linde, E., Ropke, S., Mirchandani, P.B., Larsen, A., 2016. An adaptive large neighborhood search heuristic for the electric vehicle scheduling problem. *Comput. Oper. Res.* 76, 73–83.
- Xylia, M., Leduc, S., Patrizio, P., Silveira, S., Kraxner, F., 2017. Developing a dynamic optimization model for electric bus charging infrastructure. *Transp. Res. Procedia* 27, 776–783.
- Yıldırım, Şule, Yıldız, Barış, 2021. Electric bus fleet composition and scheduling. *Transp. Res. C* 129, 103197.